1
The Structure and Reactivity of Single and Multiple Sites on Heterogeneous and Homogeneous Catalysts: Analogies, Differences, and Challenges for Characterization Methods

Adriano Zecchina, Silvia Bordiga, and Elena Groppo

1.1
Introduction

The content of this book is specifically devoted to a description of the complexity of the catalytic centers (both homogeneous and heterogeneous) viewed as nanomachines for molecular assembling. Although the word "nano" is nowadays somewhat abused, its use for catalysts science (as nanoscience) is fully justified. It is a matter of fact that (i) to perform any specific catalytic action, the selective catalyst must necessarily possess sophisticated structure where substrates bonds are broken and formed along a specific path and (ii) the relevant part of this structure, usually constituted by a metal center or metal cluster surrounded by a sphere of ligands or by a solid framework or by a portion of functionalized surface, often reaches the nanometric dimension. As it will emerge from the various chapters, this vision is valid for many types of selective catalysts including catalysts for hydrogenation, polymerization, olygomerization, partial oxidation, and photocatalytic solar energy conversion. Five chapters are devoted to the above-mentioned reactions. From the point of view of the general definition, homogeneous and heterogeneous selective catalysts can be treated in the same way. As homogeneous selective catalysts are concerned, the tridimensional structure surrounding the metal center can be organized with cavitand shape, while for heterogeneous catalysts the selectivity is the result of an accurate design and synthesis of the framework structures (often microporous and crystalline) where the sites are anchored. This is the case of zeolitic and metallorganic materials. The structure of catalytic centers in capsules and cavitands is discussed specifically in a single chapter, while the zeolitic and metallorganic catalyst are treated in two chapters. One of the intriguing aspects of catalysis science is represented by the wide recognition that the chemists usually design and prepare precursor structures and that the really "working" centers are formed after an induction period in the presence of reactants. For this reason, it is not sufficient to know as much as possible about the precursor structures and *in situ* characterization methods under operando conditions are beneficial. Catalyst characterization is consequently a relevant aspect of catalysis science and two chapters are devoted partially or totally to this problem.

Selective Nanocatalysts and Nanoscience, First Edition. Edited by Adriano Zecchina, Silvia Bordiga, Elena Groppo.

1.2
Definition of *Multiple*- and *Single-Site* Centers in Homogeneous and Heterogeneous Catalysis

1.2.1
Single-Site Homogeneous Catalysts: Prototype Examples Taken from the Literature

The usual definition of single-site molecular catalyst is a catalyst which contains a single metal center. The metal atom usually has an open-side, or an easily replaceable group, where it binds substrates and where bonds are broken and formed. A prototype well describing this definition is represented by the classic Wilkinson homogeneous catalysts for hydrogenation reactions, whose structure is represented in Figure 1.1a (shaded area). This is definitely the first example of single-site homogeneous catalyst having activity similar to that of heterogeneous counterparts [1]. It must be noted, however, that the reported structure is that of the *precursor species*. In fact, the really reactive center is universally thought to derive from the previous structure by the initial dissociation of one or two triphenylphosphine ligands to give 14- or 12-electron complexes, respectively. The elimination of the phosphine ligand generates a coordinatively unsaturated species able to

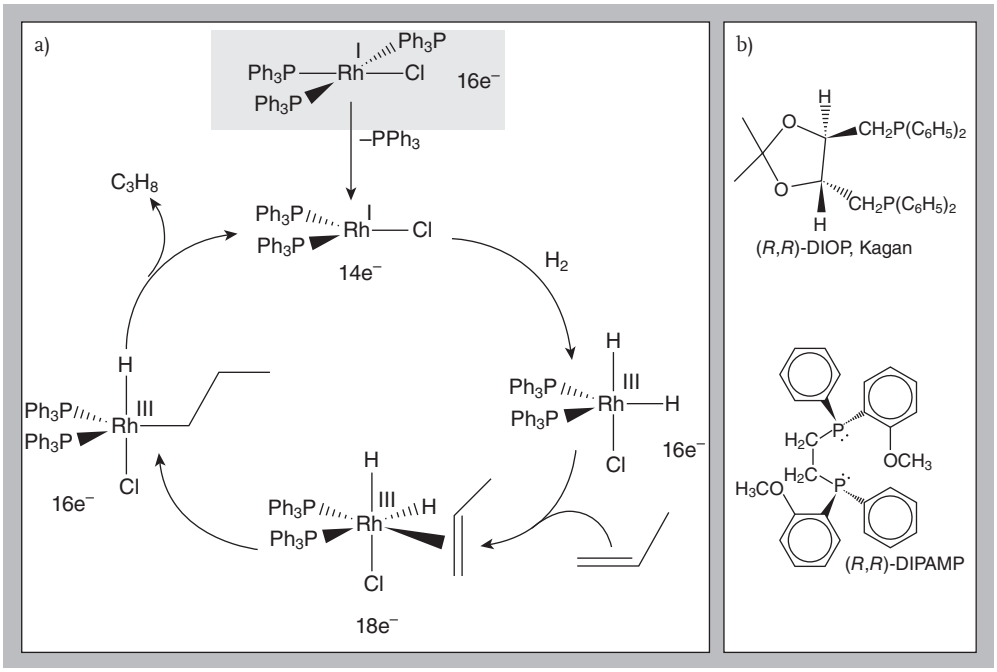

Figure 1.1 (a) Wilkinson homogeneous catalysts for hydrogenation reactions, and catalytic cycle during hydrogenation of propene. (b) Two examples of chiral ligands used instead of the phosphine groups to modify the selectivity of the Wilkinson catalyst.

dissociate the hydrogen molecule (oxidative addition of H_2 to the metal). Subsequent π-complexation of alkene, intramolecular hydride transfer (olefin insertion), and reductive elimination result in the release of the alkane product as depicted in the scheme reported in Figure 1.1a.

When the Wilkinson catalysts cycle is described, the attention is normally focused on the change in coordination and valence state of the Rh center, that is, on its electronic properties. The role of the bulky ancillary ligands (triphenylphosphine groups) is usually less considered, although it certainly plays a role in determining the selectivity in the chemospecific hydrogenation of terminal alkenes in presence of internal alkenes or other easily reducible groups [2]. That the role of ligands is central in determining the catalyst selectivity is demonstrated by the well-known fact that the use of chiral ligands instead of phosphine groups (like the chelating DIOP or DIPAMP ligands represented in Figure 1.1b) [1] transforms the Wilkinson complex into an efficient asymmetric catalyst characterized by outstanding enantioselectivity.

The role of properly tuned ancillary ligands structures covalently bonded to the metal site is not limited to the Wilkinson hydrogenation catalysts. In fact, the well-known enantioselectivity of homogeneous Ziegler type, Osborn–Schrock, and Crabtree type hydrogenation systems [3, 4] is based on the same principle. As for the Osborn–Schrock and Crabtree cationic catalysts, further role is known to be played also by the solvent molecules and by the counteranionic species, which can act as external ancillary ligands (coordinatively or electrostatically bonded) influencing both reactivity and selectivity [5, 6]. The same is valid for the role of anionic counterparts on the activity and selectivity of cationic (Wilkinson type) chiral Rh(I) catalysts [7].

A preliminary conclusion that can be derived directly from the previous considerations is that, as already underlined [6], in order to develop selectivity, the single metal center forming the core of the catalysts (where the substrates bonds are broken and formed) must be surrounded by a complex ligands framework (including the solvent molecules directly interacting with the metal center). This makes the whole structure similar to a functional nanomachine for molecular assembling. On the basis of these considerations, we can slightly modify the classical definition of selectivity [8] from "the selectivity of a catalyst is its ability to direct conversion of reactants along one specific pathway" to "the selectivity of a catalyst is its ability to direct conversion of reactants along one specific pathway also with the intervention of covalently and coordinatively bonded ancillary structures."

The considerations derived from the hydrogenation catalysts can be easily extended to other single-site catalysts. Among all, an outstanding example of single-site homogeneous catalysts is represented by the metallocene and postmetallocene family of catalysts for olefin polymerization. The first example of catalysts belonging to this family, discovered by Kaminsly [9, 10], is represented in Figure 1.2a, where M is Ti, Zr, and Hf. In the following decades, new catalysts were synthesized and tested showing a greatly improved selectivity in propene polymerization, with an increasingly sophisticated character of the ligand sphere (see, e.g., structures displayed in Figure 1.2b and c). The new structures differ from the

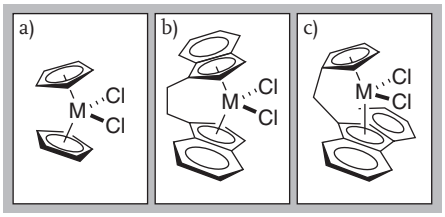

Figure 1.2 Examples of metallocene catalysts characterized by an increasingly sophisticated character of the ligand sphere (M = Ti, Zr, and Hf).

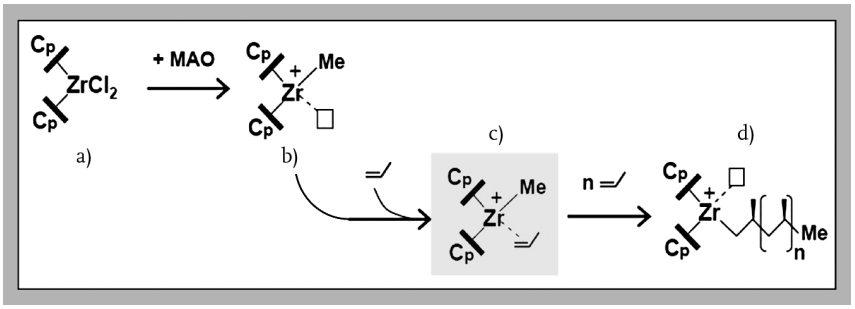

Figure 1.3 Accepted mechanism explaining the formation of the active site in case of metallocene catalysts by interaction of the metallocene precursor (a) with an activator (MAO), creation of a coordination vacancy (b), subsequent insertion of the olefinic monomer (c), followed by growth of the polymeric chain (d).

original one for the presence of an engineered ligands sphere, which confers to the catalytic center an increased rigidity and appropriately designed. The whole subject concerning the evolution of the catalysts design represents one of the most exciting pieces of research of the second half of the last century and has been excellently reviewed by Resconi *et al.* [11].

It must also be underlined that in the case of metallocene catalysts, *the represented structures are the precursors of the really active species*, which derive from them by interaction with an activator (usually MAO) following the well-known reaction reported in Figure 1.3. The resulting coordinatively unsaturated cationic structure coordinates a propene molecule and then originates the polymeric chain by a subsequent insertion reaction. It must be noticed that the complex with propene (activated complex or intermediate, shaded area in Figure 1.3) has never been experimentally observed, and consequently it must be considered as a result of mechanistic and quantum computational approaches [11].

So far, the presence of the anionic counterion has been neglected. When this is considered, the resulting ion-pair character of the catalyst is immediately emerging. As the interaction between the anion and cation forming the pair is critically dependent upon external factors such as the solvating power of the anion and the solvent polarity, it comes out that the activity and selectivity of the catalyst are not

only influenced by the structure of the covalently bonded ancillary ligand sphere, but also by external factors [5, 11, 12]. In particular, it is expected that the anion can greatly influence the insertion of the monomer molecule in the growing chain [13]. When all the involved factors are simultaneously taken into consideration, the sophisticated character of this molecular assembling nanomachine is clearly emerging.

1.2.2 Single-Site Heterogeneous Catalysts

The usual definition of single-site heterogeneous catalyst is *a catalyst constituted by a metal atom, ion, or small cluster of atoms, held by surface ligands to a rigid framework*. These sites are isolated inside the hosting structure. As the supporting solid (or rigid framework) usually exposes different faces and hence different anchoring situations, the structure of the anchored sites is usually not well known. Following this definition, the substantial difference between homogeneous and heterogeneous single sites is represented by the ligands sphere (which is accurately engineered in the first case and less defined in the second case). In the following, we will illustrate these concepts starting from cases where the anchoring structure is characterized by a definition comparable to that of the homogeneous sites, and moving to situations of increasing complexity. As previously discussed for homogenous catalysts, it will be illustrated that by appropriate surface and hosting structures engineering the selectivity of the catalyzed reactions can be tuned up to levels comparable with those of the homogeneous systems.

1.2.2.1 TS-1 and the Shape Selectivity

Among the solid frameworks which can anchor or host the catalytically active centers, zeolites and zeolitic materials occupy an outstanding position, because they are crystalline and the resulting materials have large practical applications. One of the catalytic systems where the structural situation of the metal center (Ti^{IV}) is better known is titanium silicalite (TS-1, Figure 1.4a), a catalyst which has found wide practical applications in oxidation reactions with hydrogen peroxide (Figure 1.4b) [14–18].

The precursor structure of TS-1 (i.e., the structure of the catalyst before contact with reagents) is illustrated in Figure 1.4c. It has been fully demonstrated that in the virgin samples, the Ti^{IV} centers occupy regular tetrahedral positions of the framework, because they substitute the silicon atoms. When immersed in the hydrogen peroxide water solutions, the coordination sphere of the Ti^{IV} centers expands to an octahedral situation. This is the result of the formation of the "active single-site structure" reported in Figure 1.4c, which is formed in solution by hydrolysis of ≡Si–O–Ti≡ bridges and interaction with water and hydrogen peroxide molecules. The structure of the active site under conditions approaching the reaction situation has been the subject of many investigations with physical methods such as UV-Vis, XANES, EXAFS, Raman, and FTIR spectroscopies [14–20]. When

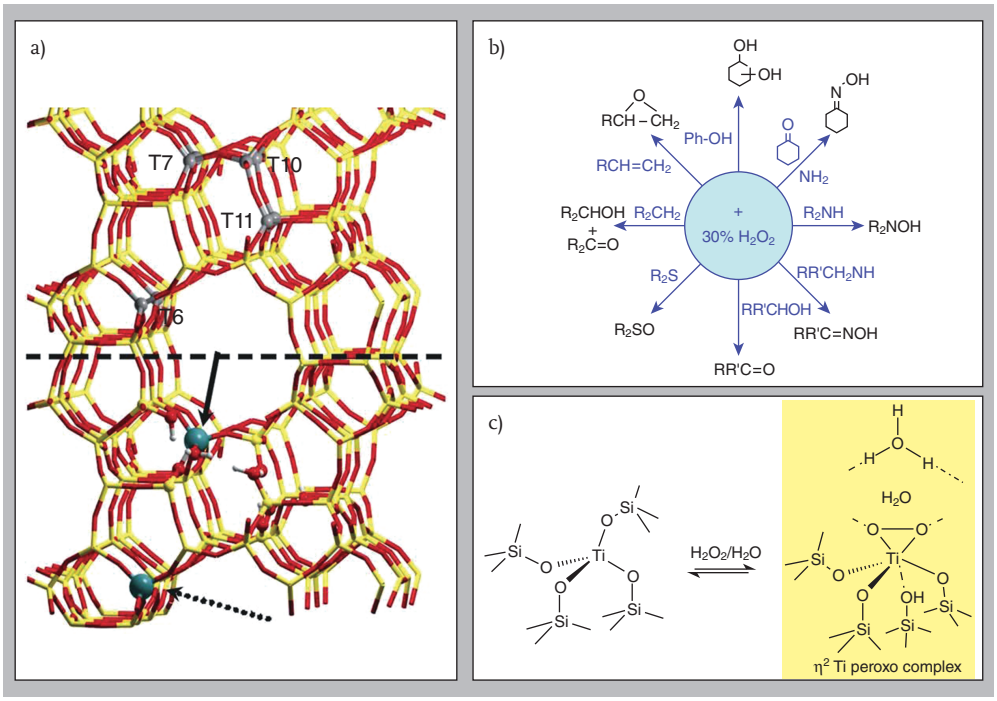

Figure 1.4 (a) Schematic representation of the preferential location of Ti atoms and Si vacancies in the TS-1 framework (upper part) and their interplay (lower part). Yellow and red sticks represent Si and O of the regular MFI lattice; green balls refer to Ti, while red and white ones to O and H of defective internal OH groups. Dotted and full arrows evidence regular $[Ti(OSi)_4]$ and defective $[Ti(OSi)_3OH]$ sites, respectively. (b) Role of TS-1 in oxidation in chemical reactions. (c) Formation of the active single-site structure by hydrolysis of ≡Si–O–Ti≡ bridges and interaction with water and hydrogen peroxide molecules.

a substrate molecule (olefin, phenol, etc.) is approaching the active center, a hydrogen-bonding interaction with the Ti–OOH group is likely to occur, followed by an oxygen transfer. In this case, the hydrogen-bonded species is one of the reaction intermediates.

The TS-1 system is interesting not only because it is one of the heterogeneous catalysts where the structure of the active sites is better known, but also because it allows to introduce the concept of shape selectivity. TS-1 catalyzes the oxidation of phenol (PhOH) to diphenol (Figure 1.4b). Not all the isomers are, however, formed: in fact, the formation of the *m*-isomer is inhibited. This is due to the shape selective character of the catalyst characterized by channels with shape not allowing the formation and diffusion of the more spatially demanding *m*-isomer. We are here in the presence of catalytic events in confined spaces, where selection of products is made on the basis of the shape of the reactants. Following the considerations already made for homogeneous single-site catalysts, the structure of the

channels can be considered as a special and new type of external ligands sphere, having no precedent in the cases illustrated in the previous section.

The shape selectivity is usually considered as belonging to the heterogeneous catalyst domain; however it is worth mentioning that, although not relevant in the previously discussed cases, the role of confinement effects is well known also in homogeneous catalysis. It is sufficient to cite the enzyme action mechanism, where the active center (often constituted by a single metal atom or by a dimer where the substrates bonds are broken and formed) is confined in a pocket or channel of the fluxional protein structure [6, 21, 22]. Furthermore, more and more examples of homogeneous catalytic systems where the active center is located in a suitably engineered pocket are known.

1.2.2.2 H-ZSM-5: A Popular Example of Protonic Zeolite

H-ZSM5 is a zeolitic material with the same MFI structure of TS-1 described above, the substantial difference being represented by the presence of Al instead of Ti in the framework. To compensate the negative charge of the framework, in correspondence of the substitutional Al atoms, a positive center must be present (alkaline ion or proton). The protonic sites protruding into the channel in correspondence of each Al atom present in the framework are fully available for interaction with shape-selected molecules penetrating the channels (Figure 1.5). As the Si/Al ratio is never less than 15, the protonic sites are isolated and consequently can behave as single-site catalytic centers in a variety of Brønsted-catalyzed reactions.

From the point of view of the isolation and structural definition, the H-ZSM5 is one of the most defined heterogenous single-site catalysts reported in the literature. The interaction of the Brønsted sites with molecules of increasing basicity has been thoroughly studied [23–25]. When the proton affinity of the base is low, the result is the formation of a hydrogen-bonded adduct. In the case of olefin/Brønsted site interaction, the formation of the hydrogen-bonded species can be followed by protonation and formation of oligomeric species with carbocationic character following the reaction path illustrated below:

$$H^+ + C_2H_4 \rightarrow (H^+ \cdots C_2H_4) \rightarrow C_2H_5^+ \tag{1.1}$$

$$C_2H_5^+ + C_2H_4 \rightarrow (C_2H_5^+ \cdots C_2H_4) \rightarrow C_4H_9^+ \tag{1.2}$$

The formation of these carbocationic species is only the initial stage of the reaction, whose final products can be more complex linear and branched olefins (like butanes), or branched and aromatic molecules. The formation step of the protonated species is thought to occur via a hydrogen-bonded intermediate. Whether this intermediate is sufficiently stable and long lived to be observed can only be decide by means of an operando experiment. This will be discussed in the following paragraph. The protonic site can also interact with methanol and ethanol giving H_2O and olefins and more complex molecules following a path similar to that illustrated above. It is thought that under reaction conditions, the real catalyst is a pool.

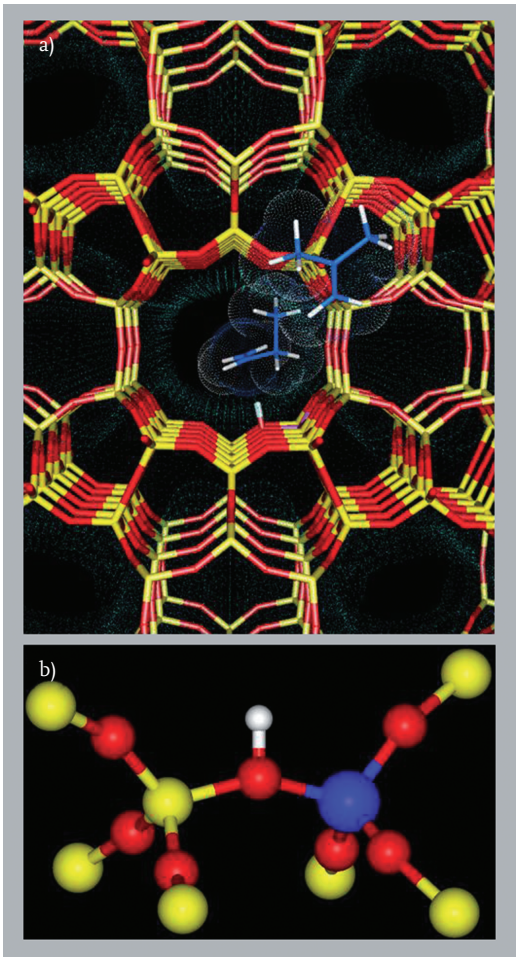

Figure 1.5 (a) Schematic representation of an MFI structure with a protonic site protruding into the main channel and interacting with shape-selected molecules penetrating the channel. (b) It shows an enlargement of the protonic site. Si, O, Al, and H atoms are represented in yellow, red, blue, and white, respectively.

In some other cases, protons cannot be considered as active sites as they are only the starting point needed for the formation of more complex carbocationic species that act as catalytic center. This is the case of methanol-to-hydrocarbons (MTH) reaction, for which the complex mechanism has been subject of numerous studies during the past 30 years [26–28]. In MTH, it has been observed a rapid conversion of methanol to dimethyl ether (DME) and water, followed by olefin formation and finally by concurrent formation of aromatics and paraffins, in agreement with thermodynamic equilibrium under the chosen conditions. Today, it is generally accepted that the MTH reaction proceeds over a hybrid site consisting

of the zeotype/zeolite lattice including the active and acidic site and an adsorbed hydrocarbon intermediate, which reacts with methanol or dimethyl ether to form a larger hydrocarbon entity, and subsequently splits off olefins. This mechanistic scheme is referred to as the so-called hydrocarbon pool mechanism [29–31]. It has been claimed that the number of methyl groups on the main methylbenzene and their protonated analogues change in consideration of the catalysts topologies (H-SAPO-34, H-ZSM-5, H-beta) [32–38]. Wide-pore H-beta zeolite stabilizes the higher methyl benzenes and gives a high selectivity to propene and butene, while the lower methyl benzene analogues in H-ZSM-5 give a high selectivity to ethene and propene [37–40]. A relevant fact that complicates MTH reaction are parallel reactions, especially olefin methylation reactions [39, 40], and fast deactivation by coke formation. In order to obtain a higher single product selectivity and coking resistance, several studies have been devoted to look for new zeolitic topologies and to consider the effect of acid strength and site density.

1.2.2.3 **The Ziegler–Natta Polymerization Catalyst**

Another single-site heterogeneous catalyst is undoubtedly the Ziegler–Natta system for olefin polymerization. After the initial discovery of the activity of the$TiCl_3/Al(C_2H_5)_2Cl$ system in olefin polymerization [41, 42], a decisive advancement in the industrial utilization of Ti^{III}-based system was obtained when Ti centers were supported on high surface area microcrystalline $MgCl_2$ [43]. Following Busico *et al.* [44] " . . . half a century after the discovery and in spite of 20 years competition with metallocenes, the classical Ziegler–Natta catalysts still dominate the industrial production of isotactic polypropylene. According to recent estimates, over 98% of installed capacity is based on $Ti/MgCl_2$ system promoted by Al-trialkyls and by electron donors adsorbed on the surface." The first step of the preparation is the adsorption of $TiCl_4$ on $MgCl_2$ surface. A common assumption is that this adsorption has epitactic character and that (100) and (110) surfaces of α-$MgCl_2$ phase are involved, resulting in the structures reported in Figure 1.6. However, the exact location of the Ti sites on the $MgCl_2$ crystal faces, edges, and corners has been matter of a debate which is still alive in the literature.

The adsorbed $TiCl_4$ is then reduced to Ti[3+] by Al-trialkyl [45]. One of the external Cl atoms bonded to Ti[3+] is then exchanged with an alkyl group R leading to the formation of the real active center where olefin polymerization is occurring. The whole process is displayed in Figure 1.7.

As for the polymerization of the prochiral propene molecule, for which the stereoselectivity is the major issue [46], the presence of suitable Lewis bases is mandatory. The role of these bases has been supposed to vary from (i) a simple poisoning effect on achiral sites present on the surface to (ii) a more direct effect (participation in the formation of the stereoselective site). The second hypothesis is favored by the observation that a clear correlation exists between the interaction enthalpy of $TiCl_4$ with the Lewis base and the catalytic efficiency [47]. Other authors [48] hypothesize that the Lewis bases interact with the $MgCl_2$ surface creating a chiral pocket around the metal center as reported in Figure 1.8 for the DPB base.

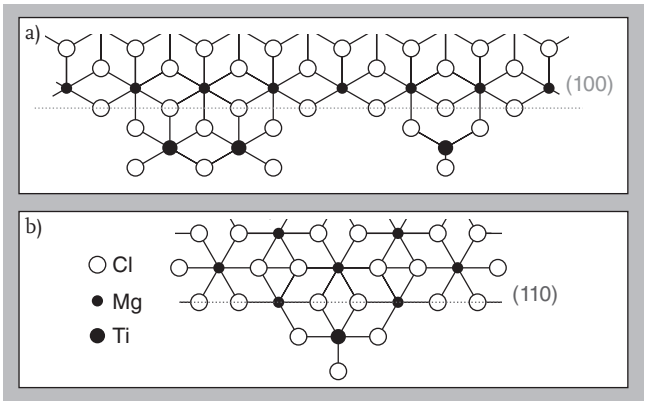

Figure 1.6 Models of $MgCl_2$ (100) and (110) surfaces and epitactic $TiCl_4$ surface adducts.

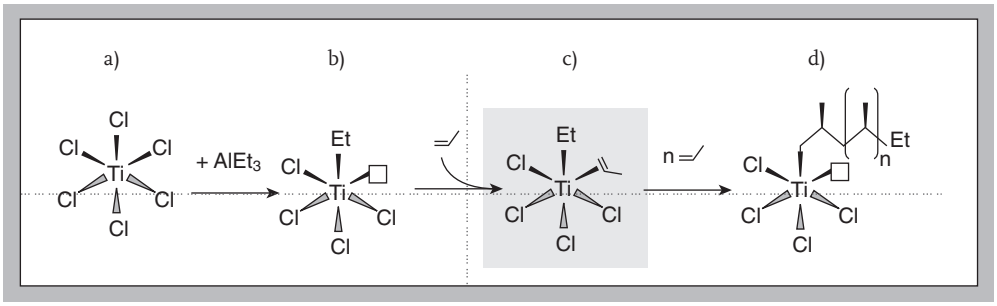

Figure 1.7 Schematic description of the formation of the really active site in case of $TiCl_4$/$MgCl_2$ Ziegler–Natta catalyst: precursor (a), coordinatively unsaturated reduced site (b), activated complex (or intermediate) with propene (c), and growing polymeric chain (d).

From the above considerations, it is clear that if on one side the single-site character of the centers is well established, on the other side the detailed structure of the active stereoselective centers is still unknown. This situation is quite common for heterogeneous catalysts, whose high efficiency and practical utility is in many cases more the result of empirical try and error approaches than of molecular engineering. It is so clear that to obtain an improved design of the catalyst, more sophisticated surface science investigations are needed. Along this line, a few contributions have appeared in the literature in the last decade [49–51], which brought new information on the structure of the sites on model Ziegler–Natta catalysts. However, the solution of the problem is still very far from completion.

1.2.2.4 The Cr/SiO_2 Phillips Catalyst for Ethylene Polymerization

The Cr/SiO_2 Phillips catalyst is by far the simplest single-site heterogeneous catalyst for ethylene polymerization synthesized so far [52, 53]. The synthesis receipt

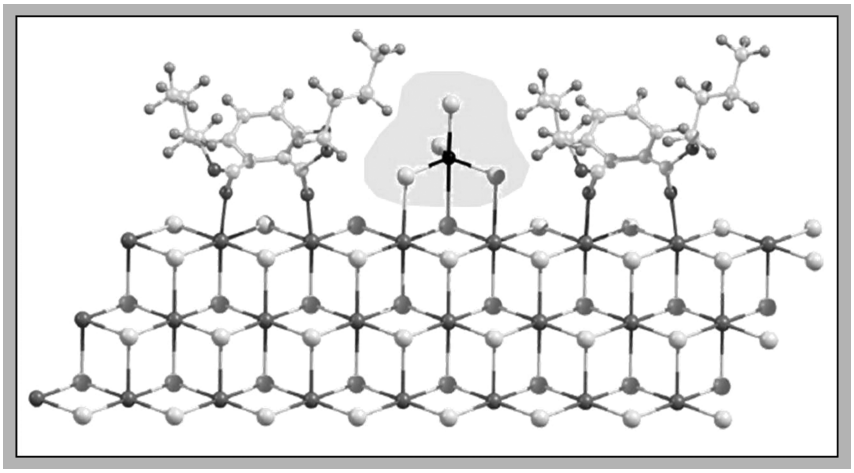

Figure 1.8 A possible model of $TiCl_4$ and DPB Lewis base co-adsorption on a $MgCl_2$ surface. Shaded area evidences the chiral pocket created by the Lewis base around $TiCl_4$.

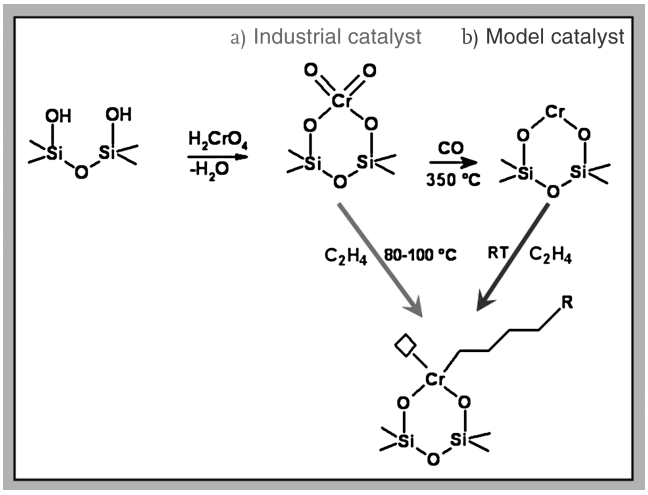

Figure 1.9 Schematic representation of the preparation and activation of Cr/SiO_2 Phillips catalyst for ethylene polymerization following the industrial (a) or model (b) route.

is very simple, as represented in Figure 1.9a. The surface hydroxyl groups of a silica particle react initially with a molecule of chromic acids forming a surface chromate. This step, which is conducted at high temperature under oxidizing conditions, does not only lead to chromate formation but is also accompanied by extensive surface dehydroxylation of the silica surface. The activation procedure can be performed in two different ways (routes a and b). Industrially (route (a))

[52], the surface chromates are treated with ethylene at about 80–100 °C; after an induction period, reduced Cr^{II} sites are formed, which are able to directly polymerize ethylene with a high efficiency. Following route (b) [53], the surface chromates are first reduced by CO (with concomitant formation of CO_2, i.e., released without interfere with the system). The so formed Cr^{II} sites are able to polymerize ethylene already at room temperature, without any induction period. In terms of productivity, the two activation ways are equivalent.

By analogy with the polymerization catalysts previously discussed, in the scheme displayed in Figure 1.9 it is arbitrarily assumed that the catalytic center contains a coordination vacancy (where the olefin molecule can insert) and a linear living hydrocarbon chain. The catalyst efficiency is comparable to that of metallocenes and Ziegler–Natta analogues. There is, however, an important difference: the catalyst cannot be used for stereospecific polymerizations. On the basis of the results illustrated for the previous catalysts, this fact can be easily understood when the structural simplicity of the ligand sphere is considered! This does not mean that the Phillips catalyst does not show selectivity properties. In fact, the molecular weight of the polymeric chain can be modulated by changing the hydroxyl groups population present on the silica surface (i.e., its surface strain), as explained by Groppo *et al*. [53, 54]. In the context of this short review, it is sufficient to recall that due to the amorphous character of the silica support, the coordination sphere of the anchored chromium ions is not completely known since, beside the two SiO^- groups linking Cr^{II} to the framework, a variable number of weaker ligands (oxygens of adjacent siloxane bridges) are present. For this reason, in this case it is better to speak of groups of single sites [55].

The Phillips catalyst is important not only because it is actually widely employed, but also because it is the only olefin polymerization catalyst where the formation of the active center does not involve the use of MAO or Al-alkyl activators. The sole reactant (ethylene) is doing the job. The questions concerning the structure of the active center and the polymerization mechanism have been the subject of many investigations [53], also with surface science methods [56–60]. The conclusion is that the initiation mechanism operative on this system, is different from that operative on homogeneous metallocenes and heterogeneous Ziegler–Natta catalysts and involves cyclic intermediates [55], as schematically shown in Figure 1.10. On this point, we shall return in the following, when *in situ* techniques under operando conditions will be illustrated. For the time being, we recall that the cyclic mechanism has been proposed also for Cr-based homogeneous dimerization and trimerization catalysts [61, 62].

1.2.3
Multiple-Site Heterogeneous Center

A multiple-site catalyst is a catalyst where the bonds breaking and forming occurs via intervention of a multitude of atoms. The hydrogenation reactions catalyzed by metal particles represent the simplest example of this type of catalyst. Figure 1.11a dis-

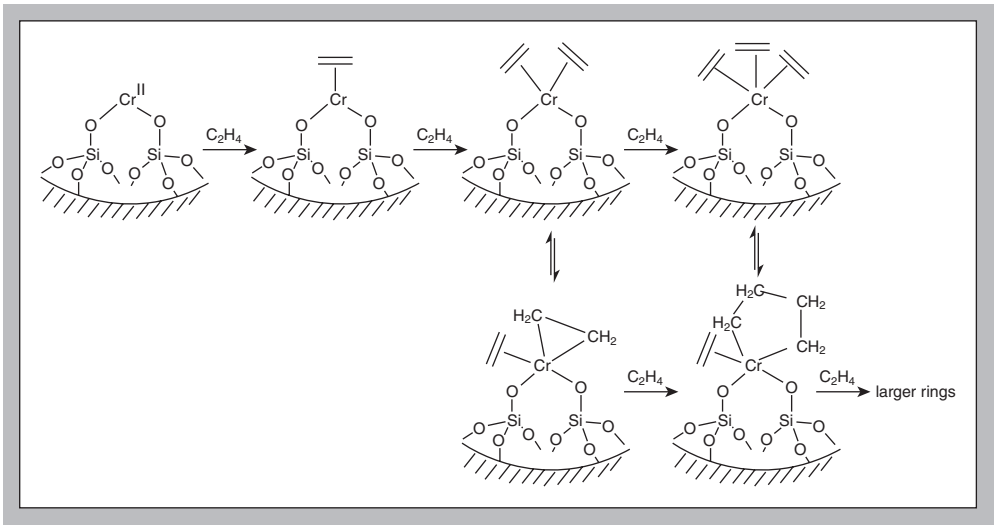

Figure 1.10 Schematic representation of the metallacycle mechanism hypothesized to explain the initiation mechanism for ethylene polimerization reaction over Cr/SiO_2 catalyst.

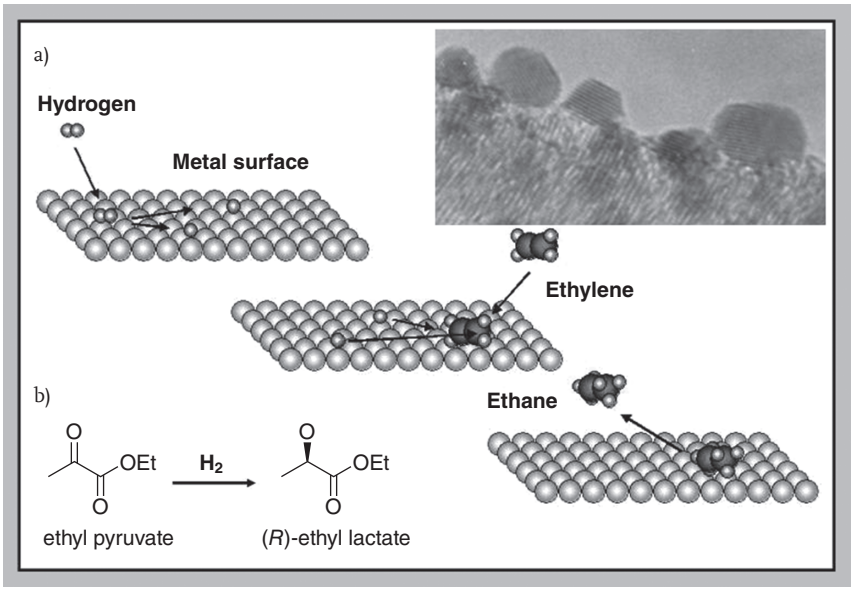

Figure 1.11 (a) Schematic representation of the ethylene hydrogenation mechanism over a metal surface. The inset shows a TEM image of supported metal nanoparticles. (b) Hydrogenation of ethyl pyruvate to ethyl lactate.

plays the hydrogenation of ethylene on a metal surface. The relevant point to be stressed here is the fact that hydrogen dissociation occurs on the surface atoms and that, due to the small surface energy barrier, the hydrogen atoms can easily migrate on the surface. This means that surface atoms not immediately adjacent to the site where ethylene is adsorbed can contribute to the reaction. In other words, a multitude of surface atoms participate to the reaction and the reaction rate is consequently very high.

Not only olefins but also other molecules containing double bonds are hydrogenated on metal surfaces such as Pd, Pt, Ru, Ir, etc. For instance, ketones can be reduced to alcohols. This is the case of ethyl pyruvate, which can be reduced to lactate in the presence of Pt particles (Figure 1.11b). The product is, however, fully racemic: this means that the metal surface is not showing enantioselectivity properties [63]. We shall see in the following that appropriate surface modification (surface engineering) can induce a satisfactory enatioselectivity, which is fully comparable with that shown by homogeneous hydrogenation catalysts.

Metal surfaces (in particular Ru) can also act as efficient catalysts for benzene hydrogenation with the formation of cycloexane (reaction (1.3) shown below) [64]. On bare metals, the formation of cyclohexene (reaction (1.4) shown below), an important feedstock for producing nylon and fine chemicals, is substantially negligible, although some information on the presence of some particle shape effect on the selectivity has been reported [65]. The absence of selectivity is mainly due to the following facts: (i) it is thermodynamically difficult to obtain cyclohexene with high selectivity since the standard free energy for cyclohexene formation by benzene hydrogenation is $-5.5\,\text{kcal mol}^{-1}$, while that for cycloexane formation is $-23.4\,\text{kcal mol}^{-1}$; (ii) the multiple-site character of the metal surface favors the multiple attack of the aromatic ring.

$$C_6H_6 + H_2 \rightarrow C_6H_{12} \tag{1.3}$$

$$C_6H_6 + H_2 \rightarrow C_6H_{10} \tag{1.4}$$

In the following, different strategies followed in literature to make the metal catalysts chemoselective for cyclohexene formation will be illustrated.

1.2.3.1 Surface Engineering and Selectivity in Heterogeneous Enantioselective Hydrogenation Catalysts

As discussed in the previous section, bare metal surfaces do not show appreciable enantioselectivity in hydrogenation reactions. In view of the increasing applicative interest of the chiral catalysis field, various strategies have been pursued to design solid enantioselective catalysts able to compete with the more established homogeneous counterparts.

Among the various proposed strategies, the most important and appealing for its synthetic potential is the strategy based on the *surface modification with chiral modifiers*. Important contributions on the subject have been published recently [66, 67]. The concept of chiral modification has been applied mainly to Pt group metals, and the used modifiers are the naturally occurring cinchona alkaloids and tartaric acid. The best example of this behavior is the hydrogenation of α-ketoesters

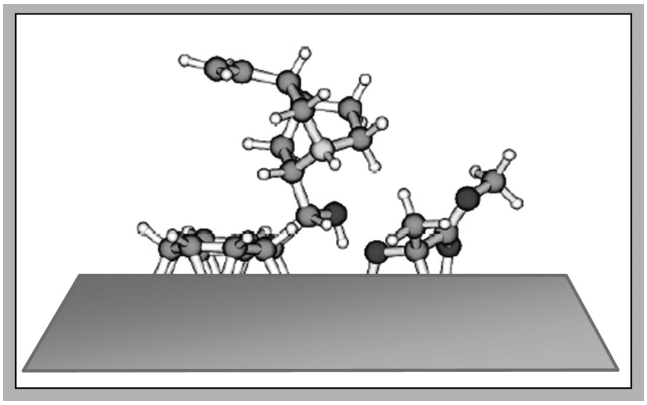

Figure 1.12 Schematic representation of a cinchonidine and methyl pyruvate adsorbed on a Pd metal particle, as modifiers to induce selectivity.

by platinum catalysts, where promotion with small amounts of cinchona alkaloids can lead to enantioselectivities exceeding 95%. The most popular mechanism by which enantioselectivity is attained is based on the idea that the cinchona modifier forms a weak hydrogen-bonded complex with the reactant and that places the reactant within its chiral pocket, forcing the carbonyl group to adopt a specific orientation. Hydrogenation of the carbonyl moiety can then lead to the preferential formation of one of the two possible enantiomers of the alcohol [68]. A representation of such interaction concerning adsorbed cinchonidine and methyl pyruvate is shown in Figure 1.12 [66, 69]. Other explanations on the effect of modifiers have been advanced. Among all, the one based on the *template model chirality* concept must be cited. Following this idea, arrays of modifiers are formed on the surface, which are responsible for the surface differentiation. The two explanations are not mutually exclusive. For the time being, it is important to stress that surface engineering at molecular level is the key point to obtain selectivity properties. Unfortunately, the level of definition of the real structure of the catalytic sites present in such heterogeneous systems is far from being completely understood and requires further efforts in surface characterization.

Another area where surface engineering is relevant and can be used to illustrate the empirical use of modifiers to increase the catalyst selectivity is the *selective hydrogenation of benzene to cyclohexene*, which is a reaction of considerable industrial utility. This reaction cannot be performed on the classical hydrogenation catalysts. Indeed it is an ascertained fact that in order to improve the selectivity of cyclohexene, the addition of surface modifiers is indispensable. These modifiers can be organic [70], inorganic [71, 72], or both [70]. So far, Ru-based catalysts modified with inorganic compounds like $ZnSO_4$ and $CdSO_4$ (or both) are the most efficient. About the function of the adsorbed modifiers in terms of local structure generated upon adsorption on the metal surface, no undisputed information is present in the literature. Even the valence state of the metal ions on the surface

of Ru is debated [70, 73–75]. It is important to remark that if Zn and Cd are present as zero-valent elements, the resulting situation should be similar to that encountered with alloys, whose catalytic activity and selectivity are known to be different with respect to that of the bare metals [68, 76]. In conclusion, the case of benzene hydrogenation to cyclohexene well illustrates a situation frequently encountered for heterogeneous catalysts that are often characterized by an undefined knowledge of the structure of the active sites, which are generated on the surface upon promotion with modifiers more as the result of empirical efforts than of molecular design.

1.2.3.2 **Is It Heterogeneous or Homogeneous? The Interplay between Homogeneous and Heterogeneous Catalysts**

The determination of the heterogeneous or homogeneous character of the active species in catalysts containing Pd, Ru, Rh, Ir complexes (and others), involved in an enormous number of reactions (like selective arene hydrogenations [77, 78], Heck- and Suzuky-type reactions [79–82]) is not so straightforward. Phan *et al.* have discussed this problem for homogeneous Pd-based catalysts [83]. As pointed out by Weddle *et al.* [78] and Finke *et al.* [84], the problem of the real nature of many homogeneous catalysts is still an open question. It is a matter of fact that in many reactions catalyzed by monometallic complexes, the presence of an induction period suggests that the employed complex is simply a precursor species and that the real catalyst is formed successively, for instance via the intervention of hydrogen (in hydrogenation reactions). For Pd-based catalysts for Heck–Suzuki reactions, some authors think that the monometallic catalysts are in equilibrium with palladium particles in stabilized colloids [81, 82], which behave as Pd reservoirs, as represented in Figure 1.13 (derived from Ref. [81]). A similar scheme has been advanced also by Reetz [79] for Heck reactions in ionic liquids.

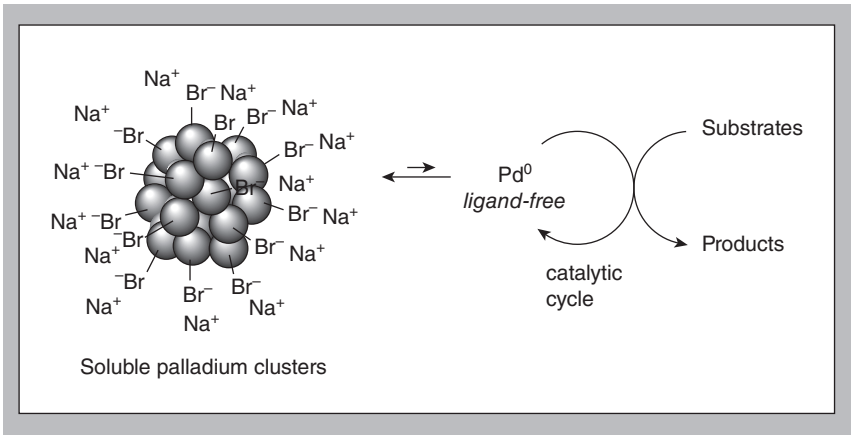

Figure 1.13 Palladium nanoclusters behaving as storage of Pd[0] in C–C bond forming reactions.

Following this hypothesis, monometallic species and clusters coexist but the active species are still the mononuclear homogeneous-type ones. On the contrary, following Reetz *et al*. [79], the catalytic events occur at defect sites (corners, steps, and kinks) of the particles. For this reason, these catalysts do not belong to the traditional area of homogeneous catalysis. The Reetz hypothesis can also be explained by hypothesizing that the Pd atoms are not free in the solution as reported in the previous scheme, but are adsorbed on the Pd surface. It is a matter of fact that an adsorbed atom, or group of atoms, on a flat surface simulates a defect site!

The discussion on this difficult point is still alive, and more sophisticated techniques and investigations are needed. A particularly important review article where the structure of hydrogenation catalysts containing not only noble metals but also Ni, Co, and Fe is discussed has been recently published [84]. As for the scope of this review, it is sufficient to underline that also for these apparently simple homogeneous catalysts, the working center appears only after an induction period (i.e., after a chemical transformation of a precursor species) and its structure looks like a very complex machine having nanotechnological character.

1.3
The Characterization Methods in Heterogeneous Catalysis (Including Operando Methods)

In the previous sections, we have seen that for many homogeneous and heterogeneous systems, the real catalyst is obtained by a well-known precursor after further reaction with promoters and/or after an induction period. The structure of the real catalyst is then more the result of reasonable hypotheses concerning the nature of the reactions occurring during the promotion/induction phase, than of direct determination by means of structural methods. In other much more complex and undefined cases, particularly involving heterogeneous systems, the real catalyst is the result of complex pretreatments and empirical surface engineering involving the use of cocatalysts and promoters. From these considerations, it is evident that the application of accurate characterization methods able to elucidate the structure of active centers and the catalytic mechanism is mandatory. However, the problem is made complex by the fact that in many cases the active centers represent a small fraction of the species present in solution (homogeneous catalysts) or on the surface (heterogeneous catalysts).

Many physical methods are used to characterize the catalytic systems. Among them, vibrational (IR and Raman), UV-Vis NIR, XANES and EXAFS, magnetic resonance (ESR and NMR), and electron (EELS, XPS, etc.) spectroscopies must be cited. The choice of the physical method which can be used to investigate the structure of the species present in a specific system depends upon the type of catalyst and reaction under investigation. The only rule which can be advanced having general validity is the following: *the characterization method must be able to*

distinguish between spectator and active species. About the mechanism of the reactions occurring at the catalytic centers, the choice of suitable spectroscopic methods under operando conditions sensitive enough to give information on the structure of elusive reaction intermediates is also mandatory. These concepts will be illustrated by three examples taken from our experience on heterogeneous catalysts.

1.3.1
TS-1-(H_2O, H_2O_2) Interaction: *in situ* XANES Experiments

As illustrated in Section 1.2.2.1, TS-1 is definitely a well-defined single-site catalyst, which operates in aqueous solution. For this reason, some characterization techniques (like FTIR) cannot be used to investigate the chemical events occurring at the catalytic site by interaction with substrates. Useful spectroscopic techniques are UV-Vis, XANES, EXAFS, and Raman spectroscopies, which are not impeded (such as FTIR) by the presence of water in the channels. In the following, only the results obtained with XANES will be briefly illustrated. As for the complementary results obtained with the other techniques, the reader is referred to the literature [14–20].

Figure 1.14 illustrates the effect on the XANES spectrum of two relevant substrates present in the TS-1 channels during the oxidation reactions: H_2O and H_2O_2. It can be noticed that in the presence of water the intense and narrow XANES peak at 4971 eV (characteristic of Ti[4+] in tetrahedral coordination) is eroded. This is due to expansion of the Ti[4+] coordination sphere from tetrahedral to octahe-

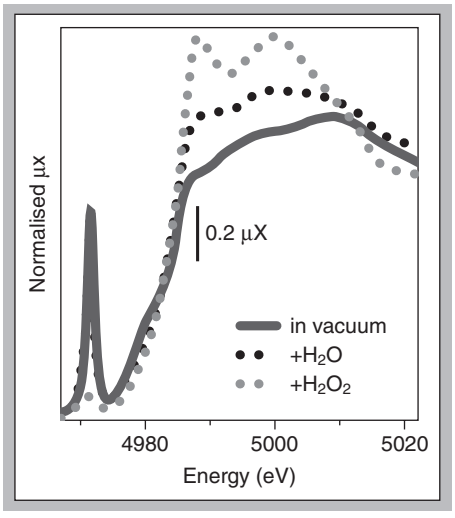

Figure 1.14 XANES spectra of TS-1 in vacuum (full gray line), immediately after contact with H_2O_2/H_2O solution (dotted gray line), and after subsequent H_2O dosage (dotted black curve).

dral, which is associated with hydrolysis of a ≡Si–O–Ti≡ bridge and coordination of H_2O to the Ti[4+] center. The process is reversible, that is, upon removal of water the original signal is restored. In the presence of H_2O_2 the erosion of the pre-edge peak is practically complete because of the formation of the final yellow colored peroxo structure reported in Figure 1.4c. Because of the presence of the solvent, in this complex the coordination sphere is complete. As the H_2O ligand is reversibly bound to the Ti[4+] center, it can be easily substituted by suitable substrates like olefins, which are then oxidized by H_2O_2. Similar conclusions have been reached by analysis of the results obtained with the other spectroscopic methods cited above. The results illustrated here can be classified as *in situ*, and well describe the chemical events occurring at the Ti[4+] center.

1.3.2 H-ZSM5-Propene Interaction: An Example of Operando Experiment by Fast Scanning FTIR Spectroscopy

As briefly described previously in Section 1.2.2.2, the interaction of olefins with the Brønsted sites present in H-ZSM5 channels leads to the formation of protonated cationic-like species. The formation of these species should occur via a short-lived hydrogen-bonded intermediate. When the interaction of H-ZSM5 with propene molecule is studied by conventional FTIR, only the spectra of the protonated product can be observed. A plausible explanation is that the reaction is so fast that the observation of the hydrogen-bonded precursor is not possible with a conventional FTIR technique. For this reason, we have performed FTIR experiment under fast scanning conditions [85]. The whole sequence of spectra reported in Figure 1.15 is lasting for 90 s. They clearly show that (i) upon interaction with propene, the Brønsted sites are immediately consumed (negative absorption band at 3610 cm^{-1}) with the formation of a broad positive absorption band at 3070 cm^{-1} due to the hydrogen-bonded species; (ii) the IR signature of the hydrogen-bonded propene is also clearly observable at 1620 cm^{-1} [ν(C=C)]; (iii) the IR absorption bands of the hydrogen-bonded precursors quickly decline and disappear completely after about 2 s; and (iv) the IR signature of the protonated species simultaneously appear. When a similar experiment is conducted in the presence of ethylene, the evolution of the hydrogen-bonded precursor is slow, thus allowing its observation with conventional IR spectroscopy [85].

Another intriguing example is represented by the propene olygomerization inside the H-MORD channels. In this case, the reaction is so fast at room temperature that even a fast scanning experiment is not sufficient to clearly observe the hydrogen-bonded precursor, which have been detected not only acting on the scanning time conditions, but also on the temperature (lower than ambient temperature) [23].

In conclusion, the results illustrated above show that spectroscopic measurements performed under real operando conditions can be of extreme utility for the elucidation of the reaction mechanisms occurring at the active centers. This utility reaches a maximum for well-defined single-site catalysts.

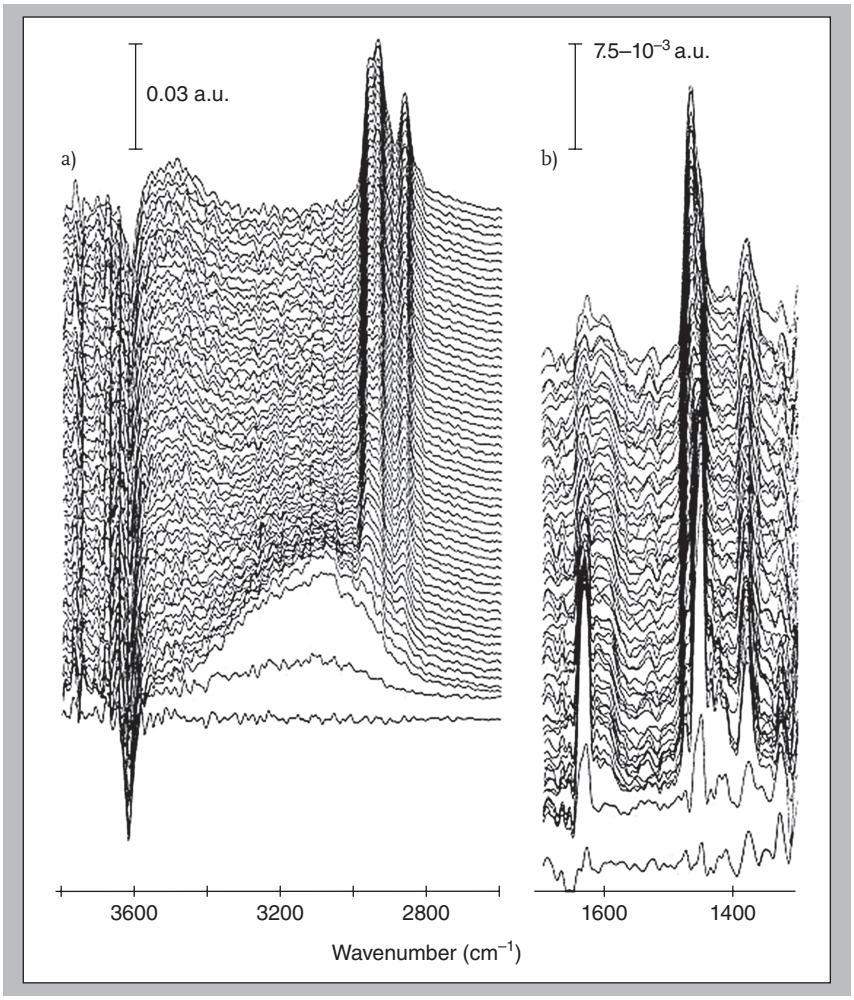

Figure 1.15 FTIR spectra, recorded in fast acquisition conditions, showing the initial stages of propene oligomerization on H-ZSM-5. The whole sequence of spectra is lasting 90 s. Part (a) reports the $\nu(CH_3)$ and $\nu(CH_2)$ region, while part (b) reports $\nu(C{=}C)$ and $\delta(CH_3)$ and $\delta(CH_3)$ region.

1.3.3
Phillips Catalyst: The Search of Precursors and Intermediates in Ethylene Polymerization Reaction by Temperature- and Time-Dependent FTIR Experiments

The major problem concerning the Phillips catalyst for ethylene polymerization (see Section 1.2.2.4) is represented by its peculiar and mysterious initiation mechanism. It is a matter of fact that the Cossee mechanism usually accepted for metallocenes and Ziegler–Natta catalysts cannot be extended to the Phillips one due to

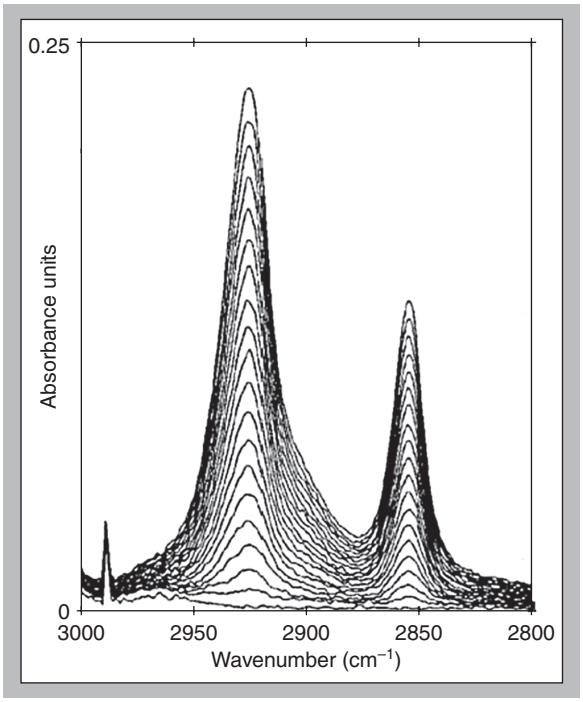

Figure 1.16 Fast scanning FTIR spectra, in the $\nu(CH_2)$ region, collected during ethylene polymerization over Cr/SiO_2 Phillips catalyst. The entire sequence of spectra is collected in only 15 s.

the absence of cocatalysts like MAO or Al trialkyls, which introduce an alkyl group into the coordination sphere of the metal center (see Figure 1.7). Previous attempts to observe the vibrational modes of terminal groups belonging to the growing polymeric chains by fast scanning IR spectroscopy failed. A typical result is illustrated in Figure 1.16, reporting a sequence of FTIR spectra of the growing polymeric chains in the 0–15 s interval. The spectra show only the IR absorption bands due to $\nu(CH_2)$ groups, without clear sign of methyl or other terminal groups. This result can have multiple explanations. Among all, two possible justifications can be advanced: (i) the reaction is so fast that the polymeric chains are always so long that the terminal groups cannot be observed; (ii) there are no $-CH_3$ or $=CH_2$ terminal groups because the mechanism is not of the Cossee or allylic type.

As completely documented in Refs. [53, 55], many hypotheses have been advanced to explain the chain initiation mechanism, and an exhaustive picture of the resulting situation is depicted in Figure 1.17. Without entering into too many details, the situation can be summarized as follows. (i) Ethylene coordinates to $Cr^{(II)}$ centers with the formation of mono-, di-, and tri- adducts. These species are the real initial precursors. The concentration of these species in the reaction conditions could be small because of the subsequent propagation steps. Consequently,

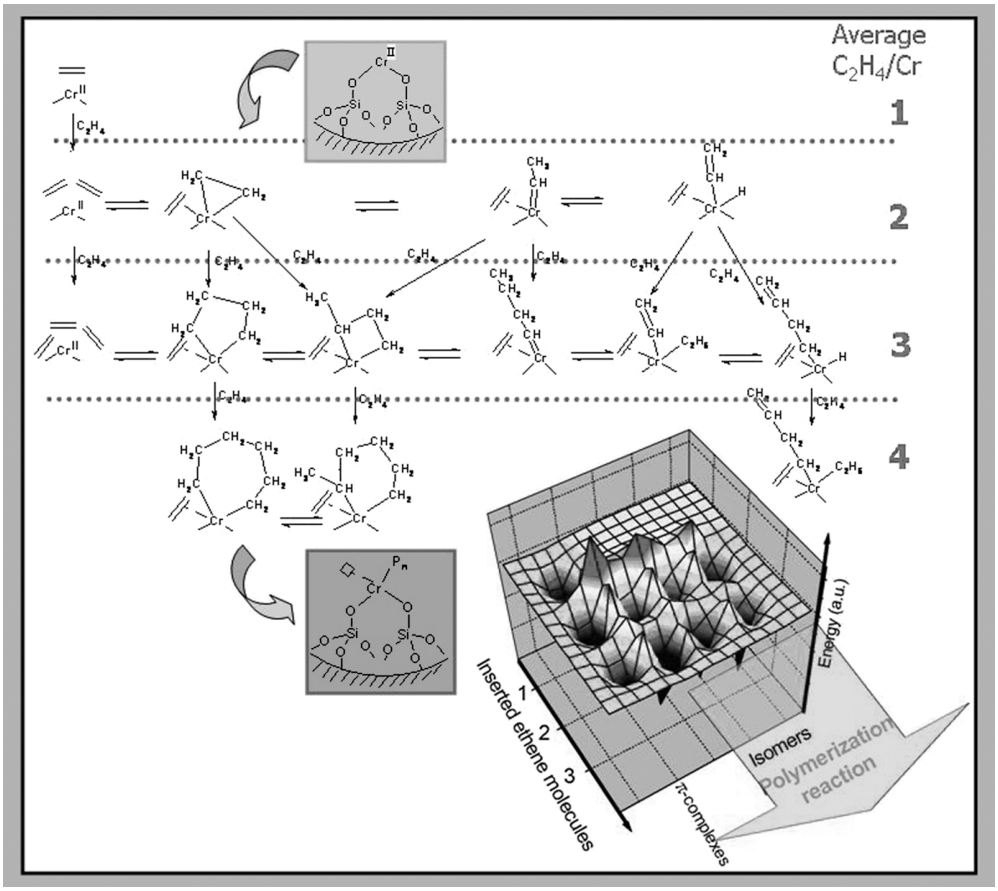

Figure 1.17 The "precursor pool" proposed in literature for the Cr(II)/SiO_2 catalyst. In the vertical direction, the evolution of the initial species upon addition of one ethylene molecule is represented. In horizontal direction, all the possible isomeric structures characterized by an average C_2H_4/Cr ratio equal to 1, 2, and 3 are reported. The inset displays a qualitative representation of the energetics of the initiation mechanisms reported in the scheme. The intermediate species are represented by potential wells of different depth, mutually separated by specific activation energy barriers of different heights. Energy values for both wells and barriers are arbitrary in depth and height, and are coded in a color scale from dark blue to red when going from negative to positive values.

they could escape detection by IR during experiments in operando conditions. (ii) The mono-ethylene adducts evolve into cyclic, ethylidene, or ethynil hydride species. These species could be in mutual equilibrium. In the presence of fast insertion and propagation reactions, their concentration under reaction conditions could also be very small and hence not detectable under the operando conditions illustrated in Figure 1.16. (iii) Ethylene insertion occurs with the formation of metallacycles, methyl-, or vinyl-terminated chains. Also these species could be in

mutual equilibrium. These species could also be directly formed starting from di- adducts. About their concentration under reaction conditions, the considerations advanced above are still valid.

Propagation can then occur by insertion into the metallacycles, or via Cossee- or allylic-type mechanisms. The metallacyclic species could be in mutual equilibrium and be directly formed from the tri-coordinated precursor. If the propagation reaction is very fast, these species are the sole which can be observed under the operando conditions illustrated in Figure 1.16. From this picture, it is evident that (i) we are dealing with a complex network of potential energy barriers (see inset in Figure 1.17) and (ii) it is difficult to make any reasonable hypothesis about the reaction intermediates that are sufficiently abundant and long lived to be observable by FTIR under operando conditions.

Considering the sequence of reactions illustrated in Figure 1.17, an obvious idea to make some precursor species observable is to decrease the propagation rate, by acting on the temperature conditions. We have so designed a particular FTIR operando experiment, named "temperature resolved FTIR spectroscopy" [55]. During this experiment, the sample temperature was gradually increased from 100 to 300 K, while the equilibrium pressure of ethylene was kept constant. The results are illustrated in Figure 1.18a. To further decrease the propagation

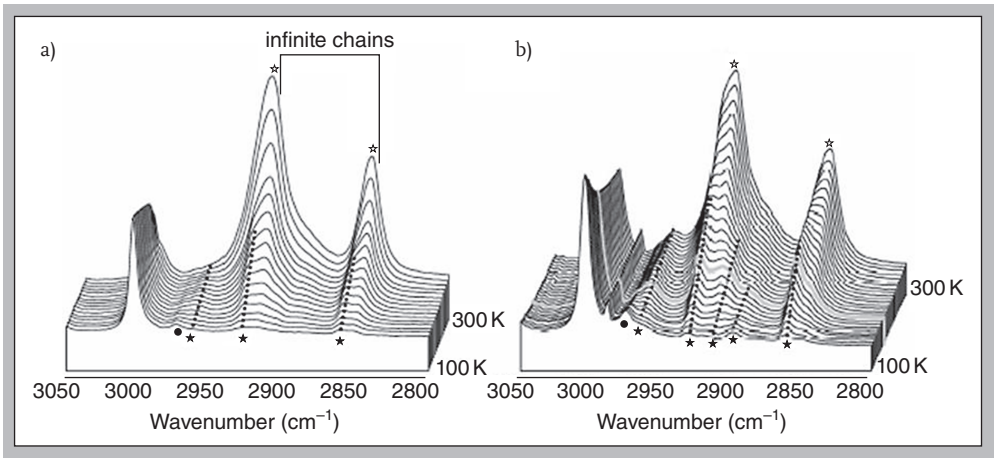

Figure 1.18 Temperature-resolved ethylene polymerization on Cr(II)/SiO_2, in the 100–300 K range, in absence (a) and in the presence of a CO poison (b). Only the C–H stretching region is shown. The first curve is dominated by the ethylene π-complexes at the highest ethylene pressure (peak at 3004 cm^{-1}) and by the almost total absence of polymerization products, which progressively appear in the successive spectra (empty stars). For comparison, the frequency position of infinite polymeric chains is also shown (black lines in (a)). The weak component at 2975 cm^{-1} (full circle) is due to the residual C_2H_4 molecules still in interaction with the silanol groups. The "anomalous bands" present in the first stages of the polymerization are evidenced by a full star and their evolution by dotted lines.

rate, the sequence of spectra illustrated in Figure 1.18b has been recorded in the presence of a small amount of CO acting as a reaction poison. When compared with the sequence illustrated in Figure 1.16, the new sequences illustrated in Figure 1.18a and b show new important features. In particular, (i) the Cr(II) $(C_2H_4)_{1,2}$ adducts can be clearly observed (IR absorption band around 3000 cm^{-1}) at low temperature and then gradually decline (as expected when the polymerization reaction starts). These species are real intermediates. (ii) New IR absorption bands which can be ascribed to terminal groups are now visible (full stars). As these "anomalous" bands cannot be assigned to methyl or vinyl terminal groups, they are assigned to CH_2 groups of small and strained cyclic species directly bonded to the Cr centers. From these results, the metallacycle mechanisms receive strong support.

From these results, it can be concluded that specifically designed operando methodologies are extremely precious to reveal the finest details about reaction intermediates and to make a choice between different reaction mechanisms. The more general conclusion deriving from the results illustrated in the previous paragraphs can be condensed as follows: (i) the physical methodology used to explore a given catalyst must be properly chosen on the basis of the nature of the catalyst to be investigated; (ii) great attention must be paid to use specifically designed operando conditions able to maximize the concentration of reaction intermediates.

1.4 Conclusions

Although the examples illustrated in the previous paragraphs have been arbitrarily selected among the numerous cases forming the homogeneous and heterogeneous catalysis realm, in our opinion they are sufficiently differentiated to be considered as representative of the structural complexity at the molecular level in the working catalytic centers. From this short review, the following conclusions can be derived:

(i) The real active center is very often the result of pretreatment and activation reactions performed on precursor structures. This explains the presence of induction periods in both homogeneous and heterogeneous reactions.

(ii) In order to build up a catalytic site highly selective for a specific reaction, the structure must be designed and engineered at a molecular level. The engineering procedure can be the result of (i) a rational approach based on the detailed knowledge of the catalyst precursor and of the subsequent reactions leading to effective formation of the active center and (ii) an empirical approach with trial-and-error character substantially based on chemical intuition. The "rational" approach is more frequent for homogeneous catalysts, while the empirical one is more frequently verified for the heterogeneous counterparts.

(iii) The role of ancillary structures surrounding the metal center is to direct the reaction along a well-defined and specific path. The more demanding in terms of selectivity is the catalyzed reaction and the more complex is the structure of the ligands sphere around the metal center. The resulting structure can be considered as a nanomachine for molecular assembling. Indeed in most cases, the ensemble constituted by the metal center, the sphere of ancillary ligands (both covalently and electrostatically bonded), and the coordinated substrates reaches the nanometer dimension.

(iv) The characterization of the structure of active centers is a difficult task and appropriate highly sensitive physical methods must be chosen. In this context, operando methods capable to distinguish between spectator species and real intermediates can be of great help.

References

1 Knowles, W.S. (2003) *Adv. Synth. Catal.*, **345**, 3.
2 Kiefer, J., Obert, K., Himmler, S., Schulz, P.S., Wasserscheid, P., and Leipertz, A. (2008) *Chemphyschem*, **9**, 2207.
3 Cui, X.H. and Burgess, K. (2005) *Chem. Rev.*, **105**, 3272.
4 Pena, D., Minnaard, A.J., Boogers, J.A.F., de Vries, A.H.M., de Vries, J.G., and Feringa, B.L. (2003) *Org. Biomol. Chem.*, **1**, 1087.
5 Macchioni, A. (2005) *Chem. Rev.*, **105**, 2039.
6 Zecchina, A., Groppo, E., and Bordiga, S. (2007) *Chem. Eur. J.*, **13**, 2440.
7 Buriak, J.M., Klein, J.C., Herrington, D.G., and Osborn, J.A. (2000) *Chem. Eur. J.*, **6**, 139.
8 Thomas, J.M. and Thomas, W.J. (1996) *Principles and Practice of Heterogeneous Catalysis*, Wiley-VCH Verlag GmbH, Weinheim.
9 Kaminsky, W. (2001) *Adv. Catal.*, **46**, 89.
10 Kaminsky, W. and Laban, A. (2001) *Appl. Catal. A*, **222**, 47.
11 Resconi, L., Cavallo, L., Fait, A., and Piemontesi, F. (2000) *Chem. Rev.*, **100**, 1253.
12 Correa, A. and Cavallo, L. (2006) *J. Am. Chem. Soc.*, **128**, 10952.
13 Busico, V., Castelli, V.V.A., Aprea, P., Cipullo, R., Segre, A., Talarico, G., and Vacatello, M. (2003) *J. Am. Chem. Soc.*, **125**, 5451.
14 Ricchiardi, G., Damin, A., Bordiga, S., Lamberti, C., Spano, G., Rivetti, F., and Zecchina, A. (2001) *J. Am. Chem. Soc.*, **123**, 11409.
15 Lamberti, C., Bordiga, S., Zecchina, A., Artioli, G., Marra, G., and Spano, G. (2001) *J. Am. Chem. Soc.*, **123**, 2204.
16 Lamberti, C., Bordiga, S., Arduino, D., Zecchina, A., Geobaldo, F., Spano, G., Genoni, F., Petrini, G., Carati, A., Villain, F., and Vlaic, G. (1998) *J. Phys. Chem. B*, **102**, 6382.
17 Bordiga, S., Coluccia, S., Lamberti, C., Marchese, L., Zecchina, A., Boscherini, F., Buffa, F., Genoni, F., Leofanti, G., Petrini, G., and Vlaic, G. (1994) *J. Phys. Chem.*, **98**, 4125.
18 Geobaldo, F., Bordiga, S., Zecchina, A., Giamello, E., Leofanti, G., and Petrini, G. (1992) *Catal. Lett.*, **16**, 109.
19 Prestipino, C., Bonino, F., Usseglio, S., Damin, A., Tasso, A., Clerici, M.G., Bordiga, S., D'Acapito, F., Zecchina, A., and Lamberti, C. (2004) *Chemphyschem*, **5**, 1799.
20 Bonino, F., Damin, A., Ricchiardi, G., Ricci, M., Spano, G., D'Aloisio, R., Zecchina, A., Lamberti, C., Prestipino, C., and Bordiga, S. (2004) *J. Phys. Chem. B*, **108**, 3573.

21 Collman, J.P., Boulatov, R., Sunderland, C.J., and Fu, L. (2004) *Chem. Rev.*, **104**, 561.

22 Merkx, M., Kopp, D.A., Sazinsky, M.H., Blazyk, J.L., Muller, J., and Lippard, S.J. (2001) *Angew. Chem. Int. Ed.*, **40**, 2782.

23 Geobaldo, F., Spoto, G., Bordiga, S., Lamberti, C., and Zecchina, A. (1997) *J. Chem. Soc. Faraday Trans.*, **93**, 1243.

24 Bordiga, S., Lamberti, C., Geobaldo, F., Zecchina, A., Palomino, G.T., and Arean, C.O. (1995) *Langmuir*, **11**, 527.

25 Zecchina, A., Bordiga, S., Spoto, G., Scarano, D., Petrini, G., Leofanti, G., Padovan, M., and Arean, C.O. (1992) *J. Chem. Soc. Faraday Trans.*, **88**, 2959.

26 Kvisle, S., Fuglerud, T., Kolboe, S., Olsbye, U., Lillerud, K.P., and Vora, B.V. (2008) *Handbook of Heterogeneous Catalysis*, vol. 6 (eds H. Ertl, H. Knözinger, F. Schüth, and J. Weitkamp), Wiley-VCH Verlag GmbH, Weinheim, Ch 13, p. 14.

27 Stocker, M. (1999) *Microporous Mesoporous Mater.*, **29**, 3.

28 Olsbye, U., Bjorgen, M., Svelle, S., Lillerud, K.P., and Kolboe, S. (2005) *Catal. Today*, **106**, 108.

29 Dahl, I.M. and Kolboe, S. (1994) *J. Catal.*, **149**, 458.

30 Lesthaeghe, D., Van Speybroeck, V., Marin, G.B., and Waroquier, M. (2006) *Angew. Chem. Int. Ed.*, **45**, 1714.

31 Song, W.G., Marcus, D.M., Fu, H., Ehresmann, J.O., and Haw, J.F. (2002) *J. Am. Chem. Soc.*, **124**, 3844.

32 Arstad, B. and Kolboe, S. (2001) *J. Am. Chem. Soc.*, **123**, 8137.

33 Song, W.G., Haw, J.F., Nicholas, J.B., and Heneghan, C.S. (2000) *J. Am. Chem. Soc.*, **122**, 10726.

34 Bjorgen, M., Bonino, F., Kolboe, S., Lillerud, K.P., Zecchina, A., and Bordiga, S. (2003) *J. Am. Chem. Soc.*, **125**, 15863.

35 Bjorgen, M., Olsbye, U., Petersen, D., and Kolboe, S. (2004) *J. Catal.*, **221**, 1.

36 Arstad, B., Nicholas, J.B., and Haw, J.F. (2004) *J. Am. Chem. Soc.*, **126**, 2991.

37 Svelle, S., Joensen, F., Nerlov, J., Olsbye, U., Lillerud, K.P., Kolboe, S., and Bjorgen, M. (2006) *J. Am. Chem. Soc.*, **128**, 14770.

38 Svelle, S., Olsbye, U., Joensen, F., and Bjorgen, M. (2007) *J. Phys. Chem. C*, **111**, 17981.

39 Svelle, S., Ronning, P.O., Olsbye, U., and Kolboe, S. (2005) *J. Catal.*, **234**, 385.

40 Bjorgen, M., Svelle, S., Joensen, F., Nerlov, J., Kolboe, S., Bonino, F., Palumbo, L., Bordiga, S., and Olsbye, U. (2007) *J. Catal.*, **249**, 195.

41 Ziegler, K., Holzkamp, E., Breil, H., and Martin, H. (1955) *Angew. Chem.*, **57**, 541.

42 Natta, G. (1956) *Angew.Chem.*, **68**, 393.

43 Soga, K. and Shiono, T. (1997) *Progr. Polym. Sci.*, **22**, 1503.

44 Busico, V., Causa, M., Cipullo, R., Credendino, R., Cutillo, F., Friederichs, N., Lamanna, R., Segre, A., and Castellit, V.V. (2008) *J. Phys. Chem. C*, **112**, 1081.

45 Busico, V., Corradini, P., De Martino, L., Proto, A., and Albizzati, E. (1986) *Makromol. Chem.*, **187**, 1115.

46 Busico, V., Cipullo, R., Monaco, G., Talarico, G., Vacatello, M., Chadwick, J.C., Segre, A.L., and Sudmeijer, O. (1999) *Macromol.*, **32**, 4173.

47 Cavallo, L., Ducere, J.M., Fedele, R., Melchior, A., Mimmi, M.C., Morini, G., Piemontesi, F., and Tolazzi, M. (2008) *J. Therm. Anal. Cal.*, **91**, 101.

48 Stukalov, D.V., Zakharov, V.A., Potapov, A.G., and Bukatov, G.D. (2009) *J. Catal.*, **266**, 39.

49 Freund, H.J., Baumer, M., Libuda, J., Risse, T., Rupprechter, G., and Shaikhutdinov, S. (2003) *J. Catal.*, **216**, 223.

50 Kim, S.H. and Somorjai, G.A. (2006) *Proc. Natl. Acad. Sci. USA*, **103**, 15289.

51 Andoni, A., Chadwick, J.C., Niemantsverdriet, J.W., and Thune, P.C. (2009) *Catal. Lett.*, **130**, 278.

52 McDaniel, M.P. (1985) *Adv. Catal.*, **33**, 47.

53 Groppo, E., Lamberti, C., Bordiga, S., Spoto, G., and Zecchina, A. (2005) *Chem. Rev.*, **105**, 115.

54 Groppo, E., Lamberti, C., Spoto, G., Bordiga, S., Magnacca, G., and Zecchina, A. (2005) *J. Catal.*, **236**, 233.

55 Groppo, E., Lamberti, C., Bordiga, S., Spoto, G., and Zecchina, A. (2006) *J. Catal.*, **240**, 172.

56 Agostini, G., Groppo, E., Bordiga, S., Zecchina, A., Prestipino, C., D'Acapito, F., van Kimmenade, E., Thune, P.C., Niemantsverdriet, J.W., and Lamberti, C. (2007) *J. Phys. Chem. C*, **111**, 16437.

57 Thune, P.C., Linke, R., van Gennip, W.J.H., de Jong, A.M., and Niemantsverdriet, J.W. (2001) *J. Phys. Chem. B*, **105**, 3073.

58 Thune, P.C., Loos, J., de Jong, A.M., Lemstra, P.J., and Niemantsverdriet, J.W. (2000) *Top. Catal.*, **13**, 67.

59 Thune, P.C., Loos, J., Lemstra, P.J., and Niemantsverdriet, J.W. (1999) *J. Catal.*, **183**, 1.

60 Thune, P.C., Loos, J., Lemstra, P.J., and Niemantsverdriet, J.W. (2000) *Abstr. Pap. Am. Chem. Soc.*, **219**, U390.

61 Ruddick, V.J., Dyer, P.W., Bell, G., Gibson, V.C., and Badyal, J.P.S. (1996) *J. Phys. Chem.*, **100**, 11062.

62 Dixon, J.T., Green, M.J., Hess, F.M., and Morgan, D.H. (2004) *J. Organom. Chem.*, **689**, 3641.

63 Heitbaum, M., Glorius, F., and Escher, I. (2006) *Angew. Chem. Int. Ed.*, **45**, 4732.

64 Hartog, F. and Zwietering, P. (1963) *J. Catal.*, **2**, 79.

65 Bratlie, K.M., Lee, H., Komvopoulos, K., Yang, P.D., and Somorjai, G.A. (2007) *Nano Lett.*, **7**, 3097.

66 Mallat, T., Orglmeister, E., and Baiker, A. (2007) *Chem. Rev.*, **107**, 4863.

67 Bonalumi, N., Vargas, A., Ferri, D., and Baiker, A. (2007) *Chem. Eur. J.*, **13**, 9236.

68 Zaera, F. (2009) *Acc. Chem. Res.*, **42**, 1152.

69 Vargas, A., Burgi, T., and Baiker, A. (2004) *J. Catal.*, **226**, 69.

70 Fan, G.Y., Li, R.X., Li, X.J., and Chen, H. (2008) *Catal. Commun.*, **9**, 1394.

71 Kluson, P. and Cerveny, L. (1995) *Appl. Catal. A*, **128**, 13.

72 Struijk, J., Moene, R., Vanderkamp, T., and Scholten, J.J.F. (1992) *Appl. Catal. A*, **89**, 77.

73 Yuan, P.Q., Wang, B.Q., Ma, Y.M., He, H.M., Cheng, Z.M., and Yuan, W.K. (2009) *J. Mol. Catal. A*, **309**, 124.

74 Yuan, P.Q., Wang, B.Q., Ma, Y.M., He, H.M., Cheng, Z.M., and Yuan, W.K. (2009) *J. Mol. Catal. A*, **301**, 140.

75 Liu, J.-L., Zhu, Y., Liu, J., Pei, Y., Li, Z.H., Li, H., Li, H.-X., Qiao, M.-H., and Fan, K.-N. (2009) *J. Catal.*, **268**, 100.

76 Serna, P., Concepcion, P., and Corma, A. (2009) *J. Catal.*, **265**, 19.

77 Lin, Y. and Finke, R.G. (1994) *Inorg. Chem.*, **33**, 4891.

78 Weddle, K.S., Aiken, J.D., and Finke, R.G. (1998) *J. Am. Chem. Soc.*, **120**, 5653.

79 Reetz, M.T. and Westermann, E. (2000) *Angew. Chem. Int. Ed.*, **39**, 165.

80 Na, Y., Park, S., Han, S.B., Han, H., Ko, S., and Chang, S. (2004) *J. Am. Chem. Soc.*, **126**, 250.

81 Alimardanov, A., de Vondervoort, L.S.V., de Vries, A.H.M., and de Vries, J.G. (2004) *Adv. Synth. Catal.*, **346**, 1812.

82 Cassol, C.C., Umpierre, A.P., Machado, G., Wolke, S.I., and Dupont, J. (2005) *J. Am. Chem. Soc.*, **127**, 3298.

83 Phan, N.T.S., Van Der Sluys, M., and Jones, C.W. (2006) *Adv. Synth. Catal.*, **348**, 609.

84 Alley, W.M., Hamdemir, I.K., Johnson, K.A., and Finke, R.R.G. (2010) *J. Mol. Catal. A*, **315**, 1.

85 Spoto, G., Bordiga, S., Ricchiardi, G., Scarano, D., Zecchina, A., and Borello, E. (1994) *J. Chem. Soc. Faraday Trans.*, **90**, 2827.